Twin-Screw Extrusion Compounding of Polypropylene/Organoclay Nanocomposites Modified by Maleated Polypropylenes

Yeh Wang, Feng-B. Chen, Kai-C. Wu

Department of Chemical Engineering, Tunghai University, Taichung, Taiwan, 407 Republic of China

Received 23 September 2003; accepted 3 December 2003
DOI 10.1002/app.20407
Published online in Wiley InterScience (www.interscience.wiley.com).

ABSTRACT: Polypropylene/organoclay nanocomposites modified with different maleic anhydride grafted polypropylene (PPgMA) compatibilizers were compounded on a twin-screw extruder. The effectiveness of the feeding sequence and compatibilizer type toward the dispersion of organoclay into PP matrix was critically studied. The composites prepared with side feed appeared to provide better dispersion and modulus improvement over that with hopper feed. The effect of PPgMA compatibilizers, including PB3150, PB3200, PB3000, and E43, with a wide range of maleic anhydride (MA) content and molecular weight was also examined. The structure was investigated with X-ray diffraction and transmission electron microscopy. The relative complex viscosity curves also revealed a systematic trend with the extent of exfoliation and showed promise for quantifying the hybrid structure of the nanocomposites. Mechanical properties were determined by dynamical mechanical analysis and tensile and impact tests. Maleated polypropylene with low-melt flow index and moderate MA content enhanced clay dispersion and resulted in significant improvement in tensile modulus of the nanocomposites. J Appl Polym Sci 93: 100–112, 2004

Key words: polypropylene; nanocomposite; maleated polypropylene compatibilizer; organoclay; twin-screw compounding

INTRODUCTION

The addition of nanoscopic fillers of high anisotropy instead of conventional reinforcing agents renders the polypropylene nanocomposites to exhibit interesting structure–property relationships and promising application perspectives. The tremendously large interface surfaces are probably responsible for the benefits such as reinforcement with low clay loading, improvement of barrier properties, refinement of dimensional stability, and enhancement of fire resistance.[1]

One of the most common nanoscopic fillers is derived from montmorillonite (MMT) clay,[2] which is found naturally in a layered silicate structure with a high surface area, about 750 m^2/g. The clay exists in a tactoid structure of 20–25 layers, which translates into an aspect ratio of about 10. Exchanging the cations in between the silicate layers with the bulkier and more organophilic cations alters the clay structure known as organoclay. This expansion of the clay layer or basal spacing makes it possible to be intercalated and exfoliated. The exfoliated clay consists of individual clay platelets of about 1 nm in thickness with an aspect ratio around 100.

The dispersion problems due to strong particle interactions of nanofillers have limited their application. Recently, melt intercalation is being recognized as a promising approach because of its ease of employing conventional polymer compounding process. Moreover, its environmental benignancy and cost effectiveness are also attractive to the compounders. Generally speaking, an interplay of entropic and enthalpic factors determines the outcome of whether an organophilic MMT (*o*-MMT) will be dispersed—intercalated or exfoliated—in a polymer.[3–5] Dispersion of MMT in a polymer requires sufficiently favorable enthalpic contribution to compensate any entropic penalties.[6] Favorable enthalpy of mixing for the polymer/*o*-MMT is achieved when the polymer/MMT interactions are stronger compared to the surfactant/MMT interactions. Although an alkylammonium surfactant adequately offers sufficient excess enthalpy for most polar polymers to promote the nanocomposite formation, in the case of polyolefinic polymers, the polymer/surfactant systems are at the theta conditions, and there is no favorable excess enthalpy to promote nanocomposite formation. Thus, the challenge with polyolefins is to design systems where the polymer/MMT interactions are more favorable than the surfactant/MMT interactions.

The usual way of increasing interactions is to increase the polymer/MMT contact area via polymer

Correspondence to: Y. Wang (yehwang@mail.thu.edu.tw).
Contract grant sponsor: National Science Council of Taiwan, Republic of China; contract grant number: NSC-92-2216-E-029-002.

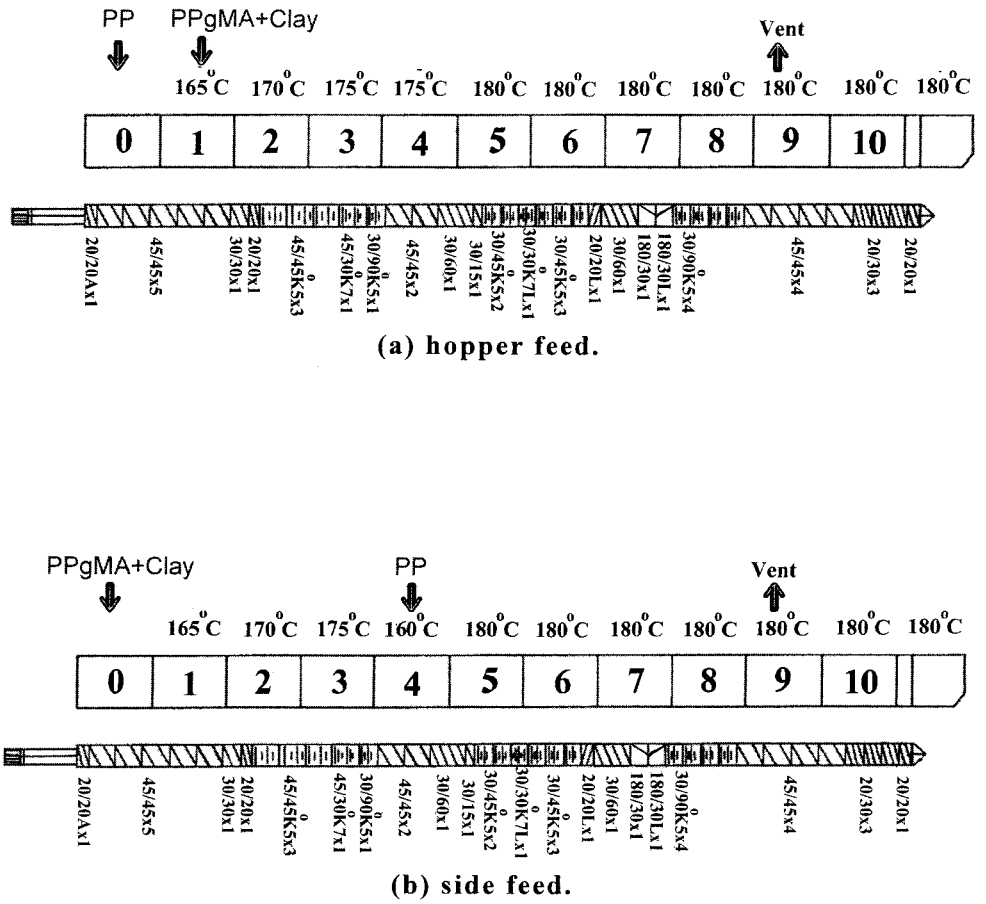

Figure 1 Screw configuration in the corotating twin-screw extruder.

functionalization. For nonpolar polymers such as polypropylene (PP), unless the organoclay is further treated with compatibilizers, applying high shear intensity alone during melt processing does not cause the clay tactoids to delaminate. Efforts were made to improve the mixing of clay in PP by using functional oligomers as compatibilizers.[7–12] High maleic anhydride (MA) content generally enhances the melt intercalation of PP oligomers into clay layers; however, it may lead to immiscibility with the PP matrix and harm the mechanical properties of the composites.[8] On the other hand, the effect of molecular weight is less clear. Most authors used low molecular weight PP oligomers to enhance the diffusion of oligomers into clay galleries[7–10]; however, high molecular weight PP oligomers gave rise to better improvement in mechanical properties.[12] In fact, there is a critical level for individual maleated PP to be incorporated into the nanocomposite. High loading of maleic anhydride grafted polypropylene (PPgMA) is detrimental to the mechanical properties, and low loading cannot reach the desirable degree of polymer/MMT interaction.

Thus far, nanocomposite development has focused on determining proper treatment of the clay to make it more compatible with the base polymer and thus improving the ease with which it can be dispersed. Certainly, clay treatment is still extremely important, but proper design and operation of the compounding system is critical. As a consequence, increasingly more attention has been given to the development of a direct compounding process that will effectively disperse and exfoliate the clay.[12–18] However, with few exceptions,[15,16] most publications are devoted to the discussion of the resultant composite properties and do not focus on the details of the compounding setup.

Indeed, the key challenge in compounding nanocomposites is to uniformly disperse clay particles that are approximately a few microns in diameter into possibly up to a million nanometer thick platelets. Previous studies[15,16] suggested that it is important to use processing equipment that is flexible in design and has the capability to combine residence time with dispersive and distributive mixing. The modular design of twin-screw extruders allows it to be configured for specific sequencing of desired unit operations (Fig. 1). The feed location and the order of feeding are important considerations in the compounding process setup. For example, the polymer and organoclay can be introduced simultaneously through the hopper at the beginning of the extruder, or the clay can be me-

TABLE I
Physical Properties of Polypropylene Matrix and Compatibilizers Under Investigation

Trade name	MI (g/10 min)	M_w (g/mol)	T_m (°C)	MA content (wt %)	T_d (°C)
PP1040	2	—	165	—	345
PB3150	20	330,000[b]	164	0.5[a]	335
PB3200	115	120,000[b]	163	1.0[a]	313
PB3000	425	—	161	1.2[a]	293
E43	1654 (180°C)	9100[a]	153	4.0[a]	161

[a] Manufacturer's data.
[b] Data from literature.[23]
MI: melt flow index, ASTM D1238, 2.16 Kg, 190°C; T_m: melting point, determined from peak value of DSC scan; T_d: onset degradation temperature, determined from TGA analysis at 1 wt % loss.

tered in separately downstream. None of these techniques is not without drawbacks.[19]

In addition to the choice of feed locations, a critical design decision is the sequencing of mixing unit operations. If pure dispersive mixing is required, then a series of wide disc kneading blocks would be necessary for providing enough shear to break up the organoclay agglomerates. However, subsequent dispersion of clay tactoids into thin platelets, owing to the penetration of polymer chain through the clay galleries, requires adequate residence time and thorough distributive mixing to completely wet the tactoids with compatibilizers. Then, finally, the host polymer would be able to peel the clay layers apart.

Although the underlying principles of intercalation process were well documented,[9,16] most studies conducted for direct melt compounding were under intuitive processing conditions within a limited range of MA content, and the effect of molecular weight of maleated PP was rarely discussed. Thus, an extensive study will be carried out by using maleated PPs of different molecular weights to elucidate the effects of molecular weight and compatibilizer loading on the clay dispersion in the PP matrix. Furthermore, important compounding parameters, such as the formulation, the feed location, and the mixing sequence are also discussed in detail. Accordingly, this study is expected to provide fundamental information required for the successful production and application development of PP-based nanocomposites and to shed some light on the interaction between the chemistry of clay modification and the compounding conditions.

EXPERIMENTAL

The isotactic PP homopolymer (Yungsox 1040) of injection grade provided by the Yung-Chia Chemical Co. (Taiwan) was used as the base polymer in this study. The density of PP was 904 kg/m^3, measured with an electronic densimeter. The organoclay was an octadecylamine (ODA)-modified montmorillonite clay (Nanomer® I.30 P) via ion–dipole interaction. Its initial basal spacing was 2.3 nm and was used as received from Nanocor. Four types of PPgMA compatibilizers were used with MA content ranging from 0.5 to 4.0 wt %. Polybond series compatibilizers were purchased from Crompton Corp. (USA) and Epolene E43 was purchased from Eastman Chemical Co. (USA). The physicochemical properties of the pristine polymer and the compatibilizers are summarized in Table I. To all the compounds, 0.2 wt % heat stabilizer (EVERNOX-10) from Everspring Chemical Co. (Taiwan) was added to prevent degradation of the polymer during compounding. PP and the stabilizer were dry-blended at room temperature after dehumidifying.

X-ray diffraction patterns for the PP nanocomposites were collected on a MacScience M18XHF-SRA diffractometer by using CuKα radiation with powdered samples. Transmission electron microscopy (TEM, Jeol JEM-1200EX) was used for direct observation of the clay dispersion in the composites. The specimen was microtomed to an ultrathin section of 70 nm for TEM analysis. The rheological characterization was carried out on a Rheometrics RDA II in the linear viscoelastic region. Dynamic mechanical analyzer (DMA, Perkin–Elmer 7e) was used to assess the mechanical performance of the composites. A Victor V90 60-ton injection molding machine was used for the preparation of tensile bars and impact specimens. Mechanical tests were performed according to tensile (ASTM D638) with a speed of 5 mm/min and notched Izod impact (ASTM D256) standards.

RESULTS AND DISCUSSION

Screw configuration for melt compounding of nanocomposites

PP/PPgMA/clay nanocomposites of different compositions were prepared on an intermeshing, corotating self-wiping twin-screw extruder. The PSM30 machine was manufactured by Sino-Alloy Machinery Inc. with D = 31.2 mm, and L/D = 45. The screw consisted of 10 segmented barrels with three kneading zones. The first one started at the second barrel with high-shear disk blocks and ended with neutral blocks. The second

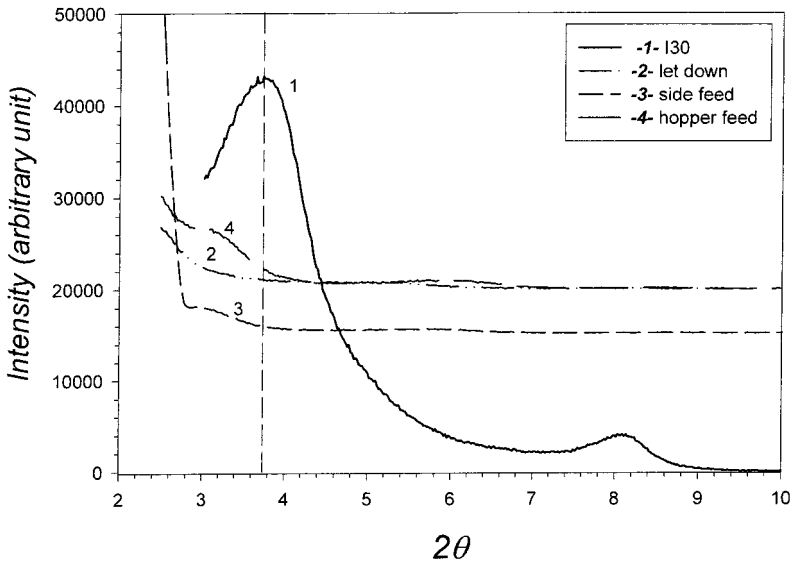

Figure 2 XRD patterns for PP/PB3150/I30 nanocomposites from different feeding sequences with a weight fraction of 80/15/5.

one started at the fourth barrel also with high-shear elements and ended with reverse elements. The third one started at the seventh barrel with a wide-pitched low-shear element. In the first and the second kneading zones, more severe shearing action is assumed because of the high-shear disk blocks and the presence of reverse elements. The reverse elements resist the forward flow resulting in an increase of the fill degree and the residence time in the mixing section. The wide-pitched element only induced gentle shearing and homogenization of the polymer melt.[16,19] Therefore, it is expected that the filler particles experience high intensity of dispersive mixing in the first and the second kneading zones and the distributive mixing dominates in the third kneading zone. The details of the screw configuration and element geometries are shown in Figure 1. A standard pelletizing die plate was at the screw end.

The major processing variables were screw speed, barrel temperature profiles, and throughput rate. After several trials, the screw speed was set at 200 rpm, and the barrel temperatures were set from 165°C at the first barrel to 180°C at the last barrel. The barrel temperature profiles are also listed in Figure 1. The screw speed and the barrel temperatures were fixed for all experimental runs, and the throughput rate was also fixed at 3.5 kg/h. Before melt compounding, PP was dried at 80°C for 24 h, and I30 was also dried at 80°C for12 h, and then dry-blended with the powdered PPgMAs. The polymer pellets and the mixed powder were then metered separately in the required proportions by using volumetric dosing units.

Feed location and feeding sequence

Various feed locations and feeding sequences were tested to achieve desirable modification of clay. Direct compounding of the nanocomposites was considered due to its simplicity.

We first fed PP upstream through the main hopper, and the premixed powder was fed downstream at the second barrel, as shown in Figure 1(a). If the premixed powder is uniformly distributed and introduced before the melting of PP, then as the base polymer experiences the pressure and requisite stress needed to induce melting, the clay is also subjected to high dispersive stresses. The process may help to break down the clay particles into smaller units. However, mixing all ingredients and melting PP and PPgMA together would interfere the wetting of clay tactoids by the compatibilizer, which is necessary for the clay layers to be delaminated from the tactoids.

In a hope to enhance the intercalation of clay layers due to the wetting and the diffusion of PPgMA into the clay galleries, we then reversed the feeding sequence. The premixed powder was fed upstream, and PP was fed downstream at the fourth barrel, as shown in Figure 1(b). Here, PPgMA will be melted in the first mixing section without the presence of the base polymer, and it is expected that the mean residence time required for mixing clay and PPgMA would be longer and the wetting of organoclay by PPgMA would be more complete. The two processes will be denoted as hopper feed and side feed in the following discussion, respectively. For comparison, a predispersed organoclay masterbatch with a weight ratio of PPgMA to I30 at 3 was first compounded. Then, the masterbatch was let down into PP to prepare composites with the preset composition.

Effect of feeding sequences on the clay dispersion

An extensive comparison is made among the composites prepared from various processes. Direct evidence

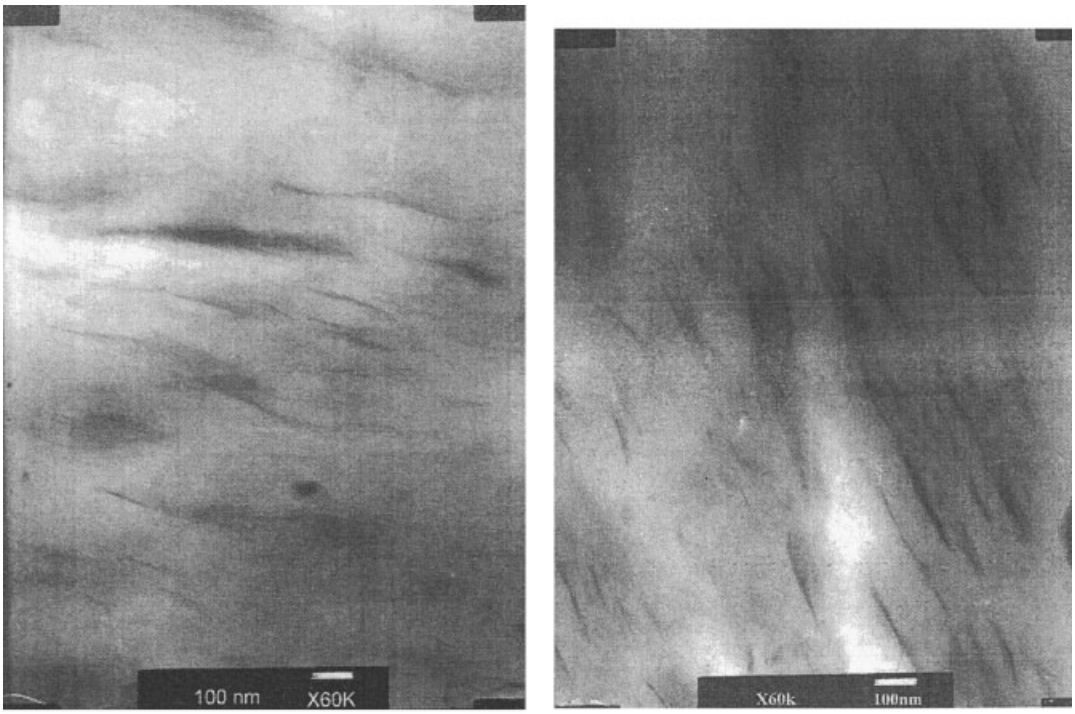

(a). Masterbatch letdown. (b). Side feed.

(c). Hopper feed.

Figure 3 TEM micrographs at ×60,000 for PP/PB3150/I30 nanocomposites from different feeding sequences with a weight fraction of 80/15/5.

of the intercalation is provided by the XRD patterns of the mixed hybrids, where diffraction peaks correspond to the d_{001} basal spacing. Figure 2 shows the XRD patterns of PP/PB3150/I30 composites with the composition of 80/15/5 by weight. It can be clearly seen that the characteristic peak of I30 is shifted to

lower angles in all samples. In addition, the XRD patterns exhibit relatively small and inapparent peaks or shoulders with a gradual increase in the diffraction strength toward low angles. It was seen that completely dispersed composites exhibit no peak but a gradual increase in the diffraction strength.[9] Therefore, the clay layers in these composites would be well exfoliated and dispersed. However, because the loading of I30 is only 5 wt %, in a partially exfoliated system, the characteristic peak may disappear simply because the fraction of unexfoliated clay particles is too small.

To observe the exfoliated structure and the dispersibility of the silicate layers, TEM images at high magnification of ×60,000 for nanocomposites prepared with different compounding processes are shown in Figure 3(a–c). Figure 3(a, b) are images for composites compounded with letdown and side feed, respectively. The gray lines are the intersections of the silicate layers of 1 nm thickness. Each layer of the clay is dispersed homogeneously in the PP matrix, although a slight amount of intercalated layers (but unexfoliated) still exists. The existence of small peaks in the XRD patterns should be attributed to these intercalated layers. On the other hand, the dark areas indicate that the clay platelets are poorly dispersed as aggregates in the continuous PP phase for the hopper-feed system [see Fig. 3(c)]. As mentioned before, when PP is fed first and melted together with the compatibilizer, the intercalation of clay by compatibilizer wetting and diffusion could be hindered by the presence of molten PP such that the clay dispersion is poor. TEM imaging is not the most ideal tool for studying dispersion in nanocomposites due to its reliance on sample uniformity. Unless the nanocomposite sample is very uniformly dispersed or unless many TEM images are taken, high magnification imagery only allows for significant analysis of a small (several microns square) area in any meaningful detail. Until nanocomposite processing methods are improved to guarantee complete sample uniformity, TEM and other imaging methods should be used in conjunction with methods such as rheology and X-ray scattering.

Besides the local technique of XRD and TEM, the rheological characterization is also a sensitive method to reveal the global state of dispersion in the composites.[20–22] The melt viscosity of these hybrid polymer nanocomposites is related to the aspect ratio of individual fillers, which is then related to the intercalation of the clay. The magnitude of the complex viscosity, $|\eta^*|$, of the composites divided by the complex viscosity of the silicate-free matrix (i.e., the blend of PP/compatibilizer) is the relative viscosity. Figure 4 presents the relative complex viscosity of the composites. It can be seen that, on one hand, composites prepared from masterbatch letdown shows the greatest enhancement in the dynamic viscosity. On the other hand, the complex viscosity of composites prepared from hopper feed shows the least enhancement. The poor dispersion of clay platelets in the composite may contribute to such low level of increase in the complex viscosity. Furthermore, the enhancement of complex viscosity is most significant in the low-frequency region for all composites, which may suggest a change from liquidlike to solidlike behavior at low frequencies.[21]

The relative storage moduli of PB3150-modified PP/I30 composites to neat PP from various compounding processes are plotted in Figure 5. In particular, the composite from masterbatch letdown exhibits

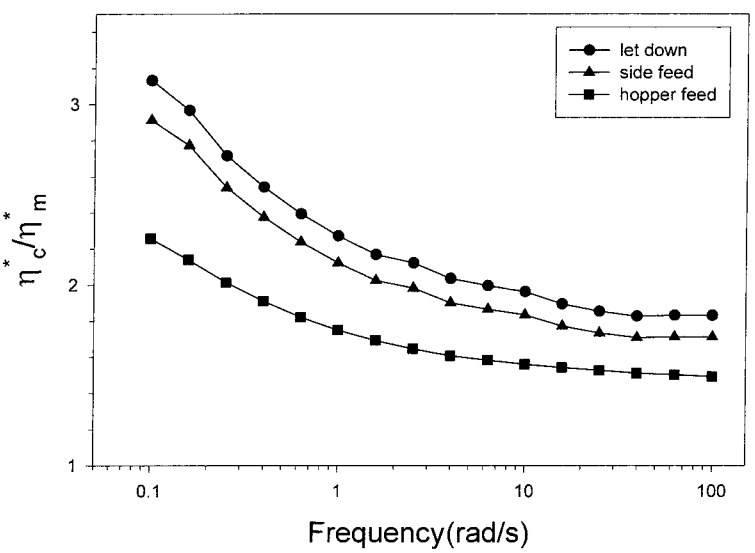

Figure 4 Relative dynamic viscosity of PP/PB3150/I30 nanocomposites from different feeding sequences to silicate-free matrix (PP/PB3150).

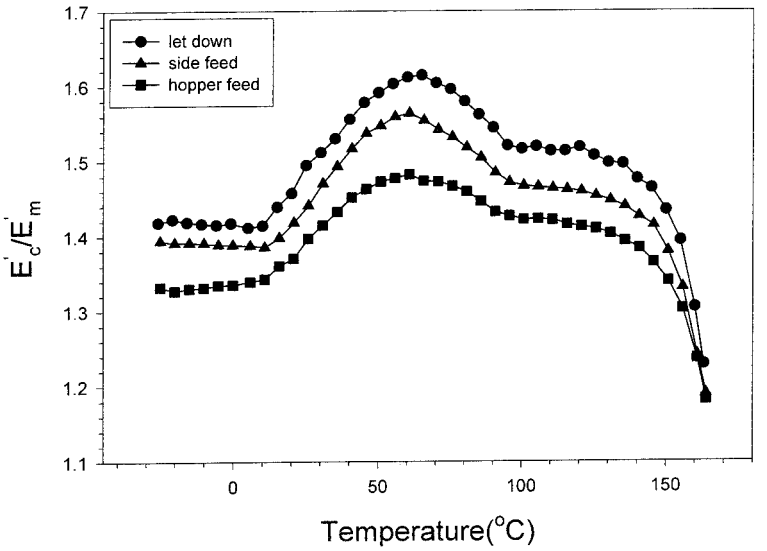

Figure 5 Relative storage modulus of PP/PB3150/I30 nanocomposites from different feeding sequences to neat PP.

nearly 1.6 times higher modulus than that of neat PP at 70°C by using only 5% of clay. This is most likely due to the fact that the improved dispersibility of clay layers compounded by masterbatch letdown. Although, as expected, the composites from hopper feed show the least improvement, apparently the relative moduli of all the clay composites are higher than unity over the whole temperature range (−30–160°C), and these are considered to be the real reinforcement effect of clays.

Next, we shall investigate the effect of feeding sequence on the PP/I30 nanocomposites modified by other compatibilizers, including PB3200, PB3000, and E43, which have lower molecular weight and higher degree of grafting than PB3150 (see Table I). Figure 6 shows the XRD patterns of modified composites through side feed and hopper feed. Regardless of feeding sequences, the characteristic peaks of I30, which are similar to that shown in Figure 1, are also shifted to lower angles, and the broadened peaks or shoulders clearly indicate a partially exfoliated PP/I30 nanocomposite. Because the XRD patterns alone seem not to be able to distinguish the difference in the degree of clay dispersion in the composites modified by various maleated polypropylenes, we then present the TEM images of nanocomposites prepared with different feeding sequences in Figures 7-9. The images of composites prepared with side feed, and modified by PB3200, PB3000, and E43, are shown in Figures 7(a)–9(a) (at ×10,000), and Figures 7(c)–9(c) (at

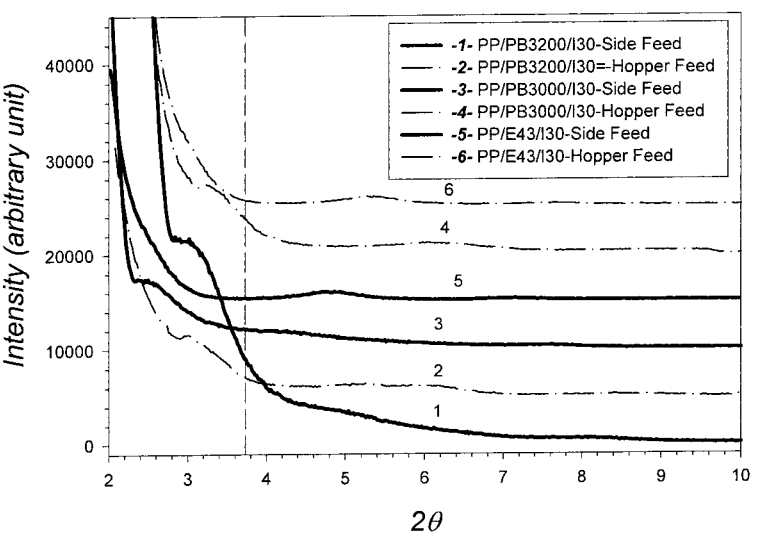

Figure 6 XRD patterns for PP/I30 nanocomposites modified with compatibilizers from hopper feed and side feed: weight fraction 80/15/5.

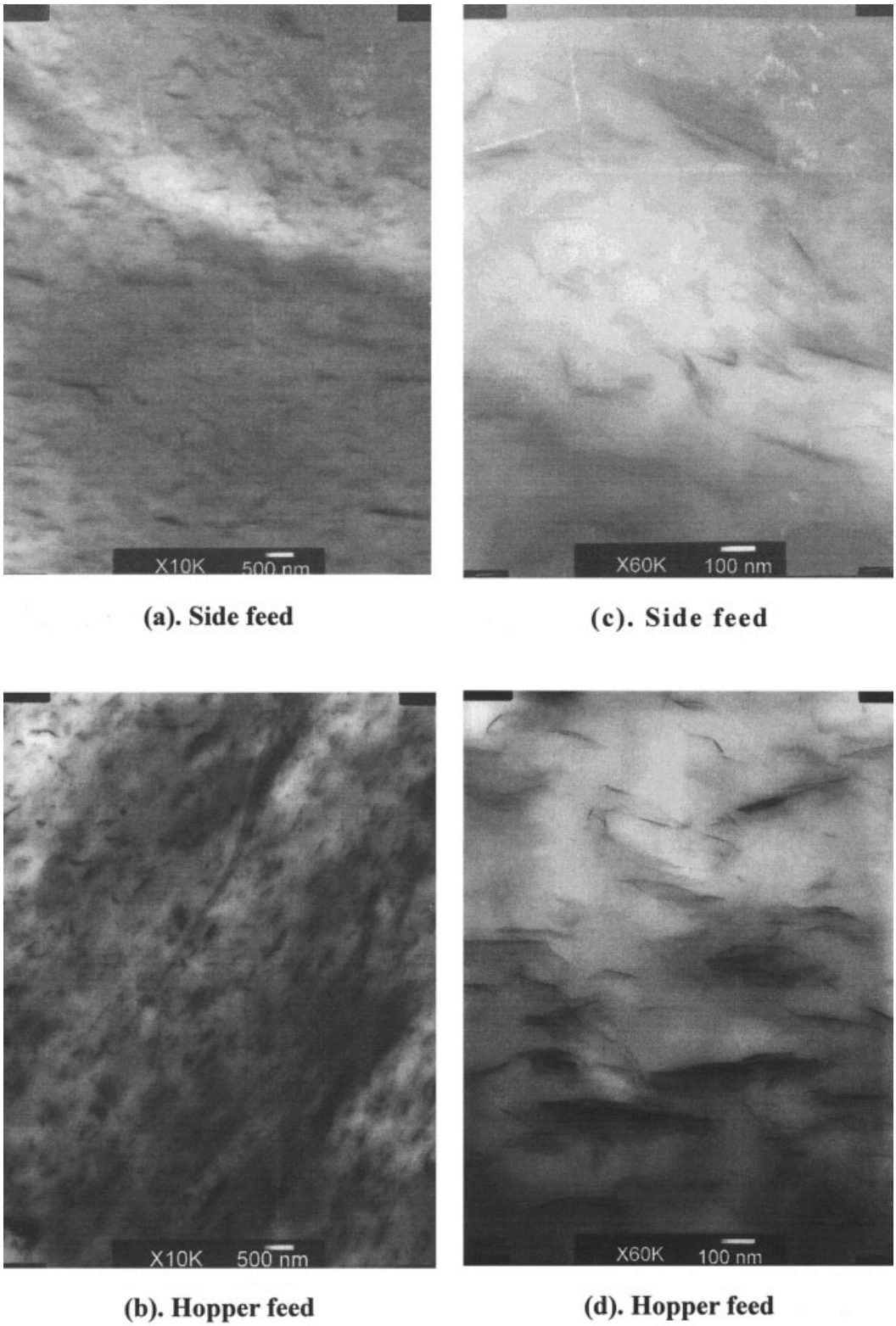

Figure 7 (a, b) TEM micrographs at ×10,000 for PP/I30 nanocomposites modified with PB3200 at 80/15/5. (c, d) TEM micrographs at ×60,000 for PP/I30 nanocomposites modified with PB3200 at 80/15/5.

×600,000), respectively. Those prepared with hopper feed are shown in Figures 7(b)–9(b) (at ×10,000), and 7(d)–9(d) (at ×60,000). The low-magnification images clearly show the existence of clay clusters in these compatibilized composite systems. The PP/E43/I30 system has the greatest number of clusters in both

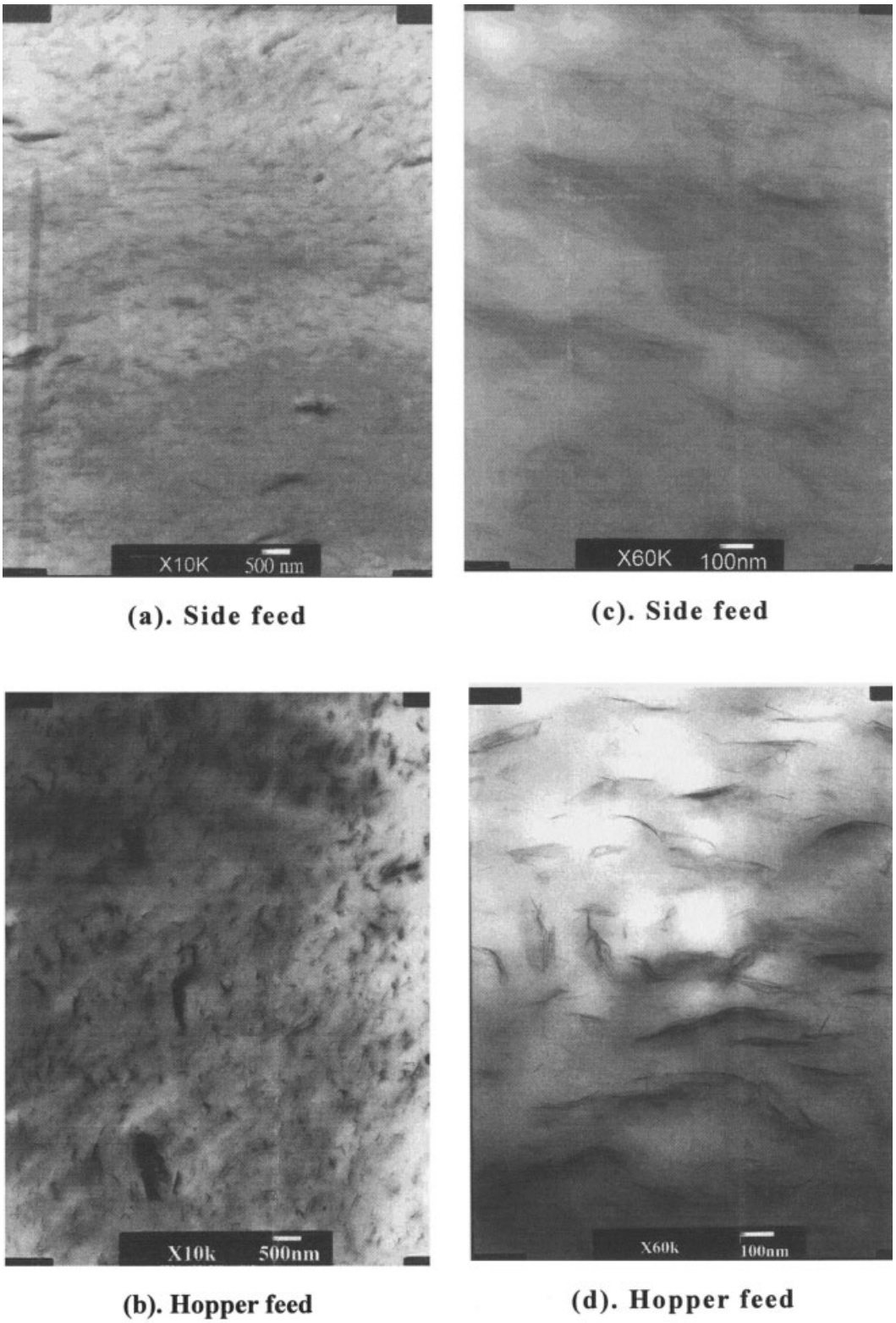

Figure 8 (a, b) TEM micrographs at ×10,000 for PP/I30 nanocomposites modified with PB3000 at 80/15/5. (c, d) TEM micrographs at ×60,000 for PP/I30 nanocomposites modified with PB3000 at 80/15/5.

side-feed and hopper-feed samples, and the side-feed samples show much less clusters than the hopper-feed samples. Note that it is difficult to observe any exfoliated clay layers at ×10,000. Thus, we need to examine the high-magnification images. These high magnification images, with similar features shown in Figure

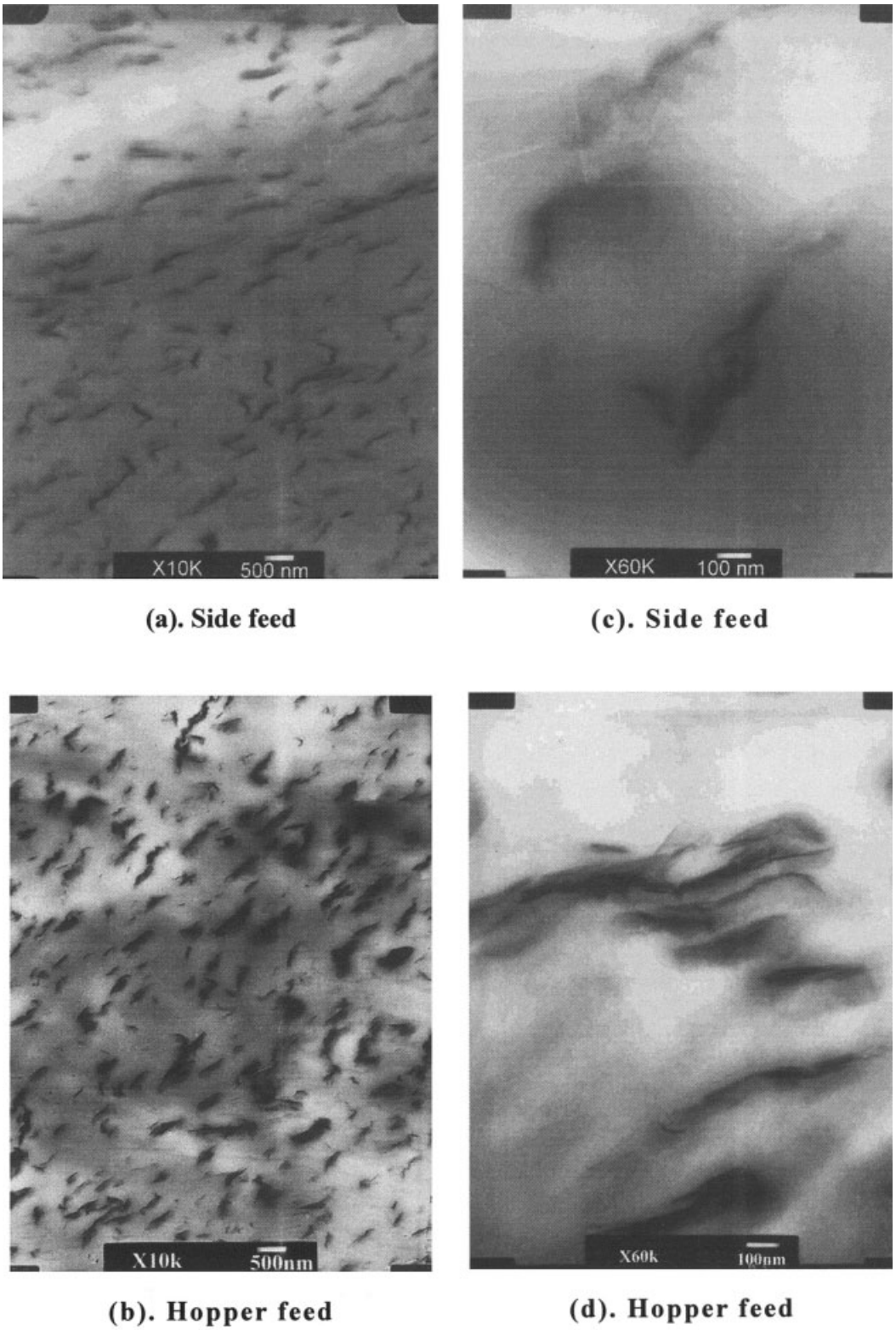

Figure 9 (a, b) TEM micrographs at ×10,000 for PP/I30 nanocomposites modified with E43 at 80/15/5. (c, d) TEM micrographs at ×60,000 for PP/I30 nanocomposites modified with E43 at 80/15/5.

3(b, c), apparently indicate better dispersion and exfoliation of I30 in the composites prepared with side feed.

We also present the relative complex viscosity of the composites in Figure 10. It can be seen that, on one hand, for composites modified with the same compatibilizer, those prepared with side feed indicate greater enhancement of the complex viscosity than that prepared with hopper feed. Moreover, it can be seen that

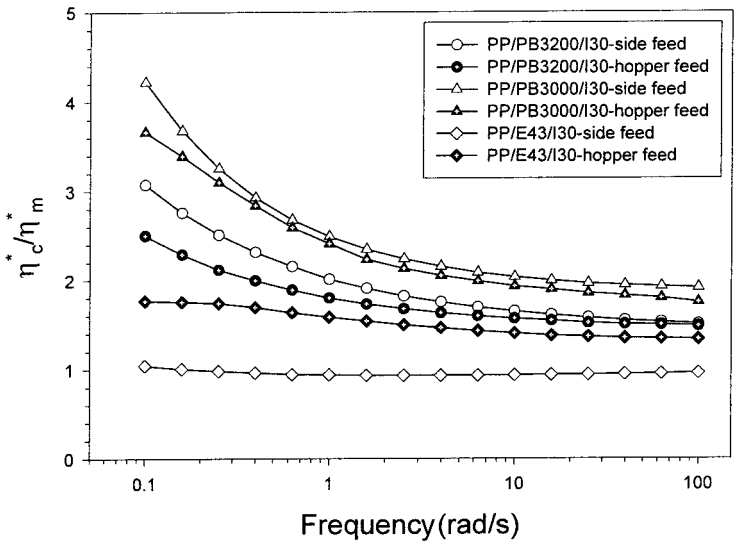

Figure 10 Relative dynamic viscosity to silicate-free matrix (PP/PPgMA) of PP/I30 nanocomposites modified with compatibilizers from different feeding sequences; weight fraction 80/15/5.

the PB3000-modified systems show the larger enhancement than any other nanocomposites. On the other hand, the complex viscosity of composites modified with E43 shows the least enhancement. The poor dispersion of clay platelets in the E43-modified composites, regardless of side feed or hopper feed, may result from the low thermal degradation temperature of E43 (see Table I).

The relative storage moduli of modified PP/I30 composites to neat PP from the two feeding sequences are plotted in Figure 11. In particular, regardless of different types of compatibilizers, the composites from side feed generally indicate higher moduli than those from hopper feed. Moreover, the E43-modified composites still exhibit the least enhancement of the storage modulus; the enhancement is simply due to the addition of clay, which is in the form of rigid particles. Note that PB3150-modified systems shown in Figure 5 exhibit the greatest enhancement among all the compatibilizers, whereas their relative complex viscosities are lower than that of PB3000-modified nanocomposites. Because the composite properties depend on the clay dispersion as well as individual component, the high molecular weight PB3150 may yield composites of higher storage modulus, even though clay dispersion is poorer than PB3000 with low molecular weight.

We finally investigate the mechanical properties of the nanocomposites. Because the focus of this study

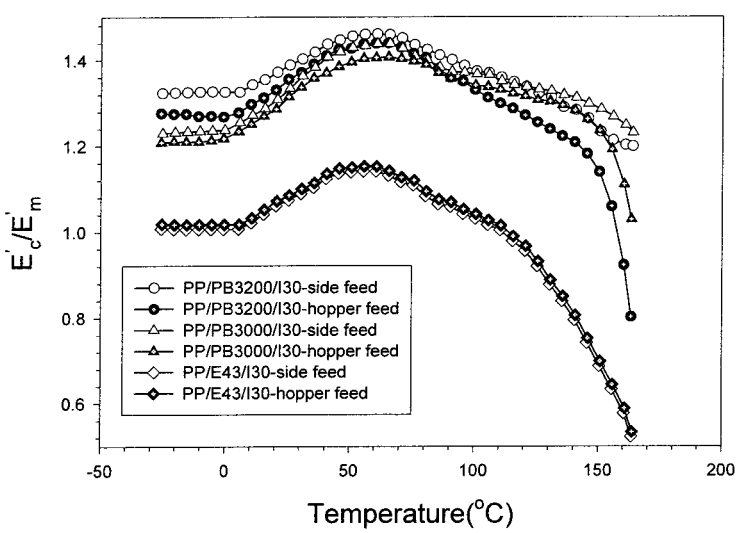

Figure 11 Relative storage modulus to neat PP of PP/I30 nanocomposites modified with compatibilizers from different feeding sequences; weight fraction 80/15/5.

TABLE II
Mechanical Properties of Modified Nanocomposites Made via Different Feeding Sequences

	Tensile modulus(MPa)		Yield strain (%)		Yield strength(MPa)		Impact strength (KJ/m^2)	
	Side	Hopper	Side	Hopper	Side	Hopper	Side	Hopper
Neat PP	—	690	—	13.3	—	20.0	—	3.3
3000	927	912	11.2	10.2	22.8	22.0	2.9	2.1
3200	1037	936	11.1	12.3	26.6	24.4	3.2	2.9
3150	1003	956	10.2	10.2	26.7	23.2	3.4	2.4
E43	1154	1108	8.3	7.8	28.3	24.8	2.3	1.9

was primarily to assess how compounding process and compatibilizer type affect clay dispersion, only limited mechanical property evaluations were made. Table II shows mechanical properties of the composites obtained, specifically tensile modulus taken at 0.3% strain, the yield strain, the yield strength, and the notched Izod impact strength. The tensile modulus was taken at 0.3% strain because it is in the elastic region for all samples; and it could be determined more unambiguously from the stress–strain curve than the initial slope at the origin. As expected, the composites prepared with side feed generally show better performance than that with hopper feed in all properties. Furthermore, the composites modified by PB3150 show the greatest magnitude in most of the mechanical properties except modulus and yield strength, which are only slightly lower than the E43-modified system. Note that the E43-modified system shows the lowest values in both yield strain and impact strength; however, it shows the highest modulus and yield strength, which is probably due to the brittle nature of the sample with a large amount of unexfoliated clay particles and inhomogeneous dispersion (see Fig. 9). Furthermore, when comparing the obtained composites with neat PP, only significant enhancement in tensile modulus and yield strength is observed. The impact strengths of all the samples are about the same level except the E43-modified system. The yield strain decreases slightly in the obtained composites modified by compatibilizers other than E43. The results indicate how both matrix modification and the compounding process have a direct influence on the mechanical properties of the obtained composites. Of course, exfoliation of clay influences properties other than modulus and strength; future articles will address these structure–property issues.

CONCLUSION

A series of PP/*o*-MMT nanocomposites modified with different types of PPgMA were melt compounded on a twin-screw extruder. The effectiveness of different feeding sequences on dispersing *o*-MMT platelets in PP was studied. The composites prepared with side feed achieve better dispersion than hopper feed, as revealed by WAXD, TEM, and dynamic melt rheology measurements. Similarly, better improvement in mechanical properties is also exhibited by composites prepared with side feed.

Effective dispersion of the clay platelets relies on both the compounding process and the choice of compatibilizer. It was found that high degree of exfoliation and dispersion of organoclay is revealed from nanocomposites modified by PPgMAs of low-melt flow index (corresponding to medium to high molecular weight) and moderate degree of grafting. Accordingly, the best mechanical properties are found in the composites modified by PB3150 with the lowest MFI. The poor dispersion of modified composites by E43, which shows the highest MFI (corresponding to low molecular weight) and the highest degree of grafting, is mainly due to its high temperature instability.

As a result, the relationship between the chemistry of compatibilizers and the proper design of compounding process should be coupled, because both might affect the exfoliation behavior and the final properties of the nanocomposites. Moreover, increasing the mean residence time through side feed generally improves the exfoliation and dispersion. Adequate residence time is required to allow the compatibilizer to enter the clay galleries and peel the platelets apart. In short, only proper combination of chemical treatment and compounding would give rise to a high degree of clay exfoliation and dispersion, which is responsible for significant enhancement of mechanical properties.

The financial support of this research by the National Science Council of Taiwan, Republic of China, under Grant NSC-92-2216-E-029-002 is gratefully acknowledged.

References

1. Gibson, A. G. Chapter 2; in Karger-Kocsis, J., Ed.; Polypropylene: Structure, Blends and Composites; Chapman & Hall: London, 1995; Vol. 3, pp. 71–112.
2. van Olphen, H. Clay Colloid Chemistry; Krieger Publishing: Melbourne, FL, 1977.
3. Vaia, R. A.; Giannelis, E. P. Macromolecules 1997, 30, 7990–7999.

4. Vaia, R. A.; Giannelis, E. P. Macromolecules 1997, 30, 8000–8009.
5. Balazs, A. C.; Singh, C.; Zhulina, E. Macromolecules 1998, 31, 8370–8381.
6. Vaia, R. A.; Ishii, H.; Giannelis, E. P. Chem Mater 1993, 5, 1694–1696.
7. Kurokawa, Y.; Yasuda, H.; Kashiwagi, M.; Oya, A. J Mater Sci Lett 1997, 16, 1670–1672.
8. Kato, M.; Usuki, A.; Okada, A. J Appl Polym Sci 1997, 66, 1781.
9. Kawasumi, M.; Hasegawa, N.; Kato, M.; Usuki, A.; Okada, A. Macromolecules 1997, 30, 6333.
10. Hasegawa, N.; Kawasumi, M.; Kato, M.; Usuki, A.; Okada, A. J Appl Polym Sci 1998, 67, 87–92.
11. Oya, A.; Kurokawa, Y.; Yasuda, H. J Mater Sci 2000, 35, 1045–1050.
12. Reichert, P.; Nitz, H.; Klinke, S.; Brandsch, R.; Thomann, R.; Mülhaupt, R. Macromol Mater Eng 2000, 275, 8–17.
13. Hasegawa, N.; Okamoto, H.; Kato, M.; Usuki, A. J Appl Polym Sci 2000, 78 1918–1922.
14. Reichert, P.; Hoffmann, B.; Bock, T.; Thomann, R.; Mülhaupt, R. Macromol Rapid Commun 2001, 22, 519–523.
15. Cho, J. W.; Paul, D. R. Polymer 2001, 42, 1083–1094.
16. Dennis, H. R.; Hunter, D. L.; Chang, D.; Kim, S.; White, J. L.; Paul, D. R. Polymer 2001, 42, 9513.
17. Nam, P. H.; Maiti, P.; Okamoto, M.; Kotaka, T.; Hasegawa, N.; Usuki, A. Polymer 20001, 42, 9633–9640.
18. Wang, Y.; Chen, F.-B.; Wu, K.-C. J Compos B: Eng to appear
19. Wang, Y. Rapra Rev Rep 2000, 10, 32.
20. Solomon, M. J.; Almusallam, A. S.; Seefeldt, K. F.; Somwangthanaroj, A.; Varadan, P. Macromolecules 2001, 34, 1864.
21. Ren, J.; Silva, A. S.; Krishnamoorti, R. Macromolecules 2000, 33, 3379.
22. Marchant, D.; Jayaraman, K. Ind Eng Chem Res 2002, 41, 6402–6408.
23. Wang, H.; Zeng, C.; Svoboda, P.; James Lee, L. 59th ANTEC Proceedings; Society of Plastics Engineers: Dallas, TX; 2001; pp. 2203–2207.